

## Effect of Deformation on Damping Capacity and Microstructure of Fe-22%Mn-8%Co Alloy

Young-Seob Seo<sup>1</sup>, Young-Kook Lee<sup>1,\*</sup> and Chong-Sool Choi<sup>2</sup>

<sup>1</sup>Department of Metallurgical Engineering, Yonsei University, Seoul 120-749, Korea

<sup>2</sup>Research Institute of Iron and Steel Technology, Yonsei University, Seoul 120-749, Korea

Effect of deformation on damping capacity and microstructure of Fe-22%Mn-8%Co alloy has been investigated. The  $\gamma \rightarrow \varepsilon$  stress-induced martensitic transformation occurs during deformation in the alloy. The amount of  $\varepsilon$  martensite increases rapidly up to 5% deformation, and gradually increases with further deformation. The damping capacity of the alloy exhibits a maximum at around 5% deformation, and decreases with further deformation in spite of the increase in  $\varepsilon$  martensite content. The deterioration of damping capacity beyond 5% is ascribed to the dislocations introduced during deformation, which obstruct the movement of damping sources of the alloy.

(Received February 4, 2005; Accepted April 6, 2005; Published June 15, 2005)

**Keywords:** damping capacity, deformation, iron-manganese-cobalt, epsilon martensite

### 1. Introduction

In previous studies,<sup>1-4)</sup> some of the authors have reported that Fe-Mn alloy undergoing  $\gamma(\text{fcc}) \rightarrow \varepsilon(\text{hcp})$  martensitic transformation possesses a high damping capacity, which is strongly dependent on the amount of  $\varepsilon$  martensite. Recently, other alloys<sup>5-9)</sup> such as Fe-Ru, Co-Ni, Co-Mn and Fe-Cr-Mn, which experience the same martensitic transformation ( $\gamma \rightarrow \varepsilon$ ), were reported to show the high damping capacities like Fe-Mn system, and it was suggested that the damping capacities of the  $\gamma \rightarrow \varepsilon$  martensitic alloys are attributed to the movement of the stacking fault boundary in  $\varepsilon$  martensite,  $\varepsilon$  martensite variant boundary and  $\gamma/\varepsilon$  interface, in single or multiple.<sup>1-4)</sup>

In the present study, cobalt (8% in mass) which is known to reduce the stacking fault energy of the austenite phase in Fe-based alloys,<sup>10)</sup> was added to Fe-22%Mn, and the cold-rolling was carried out on the alloy at room temperature to increase the volume fraction of  $\varepsilon$  martensite by the stress-induced martensitic transformation. Then the damping capacity and microstructure of the alloy were investigated as a function of deformation degree.

### 2. Experimental Procedures

An Fe-22%Mn-8%Co alloy (in mass%) was melted in a vacuum by means of a high frequency induction furnace, and was cast into a metallic mould. The ingot of about 4 kg was homogenized in a protective atmosphere at 1273 K for 24 h, and was hot-rolled to bars with a diameter of about 13 mm. From the bars, the specimens for microstructural observation, X-ray diffraction test, and damping capacity measurement were prepared by rolling and machining. All the specimens were solution treated at 1273 K for 30 min, and were subsequently quenched into water of room temperature or subzero treated at liquid nitrogen (77 K). Cross-rolling at room temperature was carried out on the quenched specimens to increase the amount of  $\varepsilon$  martensite by stress-induced martensitic transformation without a development of pre-

ferred orientation.

The damping capacity was measured in a logarithmic decrement ( $\delta$ ) at room temperature as in the previous study,<sup>8)</sup> using a rectangular-type cantilever specimen (120 mm  $\times$  12 mm  $\times$  1.3 mm) freely vibrating in a flexural mode with about 120 Hz.

The specimens for optical microstructural observation were electro-polished in a solution of 10% HClO<sub>4</sub> + 90% CH<sub>3</sub>COOH, and etched with a solution of 60 mL HCl + 15 mL HNO<sub>3</sub> + 15 mL CH<sub>3</sub>COOH + 15 mL H<sub>2</sub>O. Foils for transmission electron microscopy (TEM) were jet-polished in a solution of 10% HClO<sub>4</sub> + 90% CH<sub>3</sub>COOH, and then observed in a JEOL JEM-200CX operating at 200 kV.

The volume fraction of  $\varepsilon$  martensite was determined by measuring the integrated intensities of  $\varepsilon$  (10-1) and  $\gamma$  (200) X-ray diffraction peaks.<sup>11,12)</sup>

### 3. Results and Discussion

Figure 1 shows X-ray diffraction patterns of the alloy before and after deformation. Two kinds of diffraction line corresponding to  $\gamma(\text{fcc})$  and  $\varepsilon(\text{hcp})$  phases are seen in the deformed specimen as well as the undeformed specimen. This indicates that only  $\gamma \rightarrow \varepsilon$  martensitic transformation occurred during deformation in Fe-22%Mn-8%Co alloy, even though two kinds of stress-induced martensitic transformation,  $\gamma \rightarrow \varepsilon$  and  $\varepsilon \rightarrow \alpha'(\text{bcc})$ , were reported to occur in Fe-Mn binary system.<sup>13)</sup>

The optical microstructures of the cold-rolled alloy are shown in Fig. 2. All the structures consist of  $\varepsilon$  (dark plate) and  $\gamma$  (white part). It is seen that the amount of  $\varepsilon$  martensite increases with increasing deformation degree. It is noticeable that the  $\varepsilon$  martensite plates are clearly observed up to 5% deformation, but when the specimens are deformed above 10%, the microstructures are heavily distorted and the distinction between  $\gamma$  and  $\varepsilon$  phases becomes difficult.

The volume fractions of  $\varepsilon$  and  $\gamma$  phases were determined by measuring the integrated intensities of X-ray diffraction lines,  $\varepsilon$  (10-1) and  $\gamma$  (200), using the following equations:<sup>11,12)</sup>

\*Corresponding author: yklee@yonsei.ac.kr

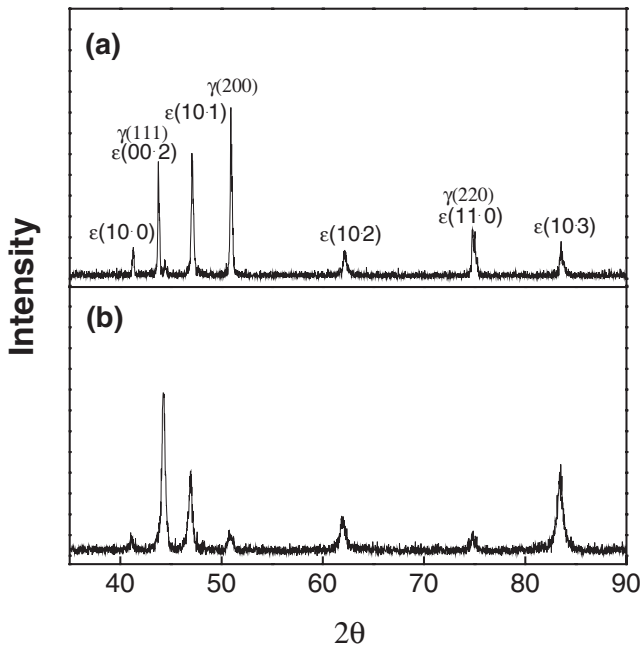


Fig. 1 X-ray diffraction patterns of Fe-22%Mn-8%Co alloy before and after deformation (Cu-K $\alpha$  radiation). (a) 0%, (b) 30%.

$$V_{\varepsilon} + V_{\gamma} = 1 \quad (1)$$

$$\frac{I_{\gamma}}{I_{\varepsilon}} = \frac{R_{\gamma}}{R_{\varepsilon}} \times \frac{V_{\gamma}}{V_{\varepsilon}} \quad (2)$$

$$R = \frac{1}{v^2} \cdot F^2 \cdot P \cdot (L) \cdot e^{-2M} \quad (3)$$

where  $V$  is volume fraction of each phase,  $I_{\varepsilon}$  and  $I_{\gamma}$  are the integrated intensities of specific diffraction lines of  $\varepsilon$  and  $\gamma$  phases,  $R_{\varepsilon}$  and  $R_{\gamma}$  correspond to  $R$  in eq. (3) for  $\varepsilon$  and  $\gamma$  phases respectively, which is determined by the following terms:  $v$  is the unit cell volume,  $F$  the structure factor,  $P$  the multiplicity factor,  $(L)$  the Lorentz polarization factor and  $e^{-2M}$  the temperature factor. As for the factors in eq. (3), the values suggested by Cullity<sup>14)</sup> were assigned.

Figure 3(a) shows a plot of  $\varepsilon$  martensite content which was measured by X-ray diffraction method versus the reduction in thickness. It is observed that the amount of  $\varepsilon$  martensite increases rapidly up to 5%, and increases gradually with further deformation. Although cross-rolling was carried out with 2% reduction in thickness per pass in order to suppress texture development, the texture was developed in some degree in the specimens subjected to high deformation

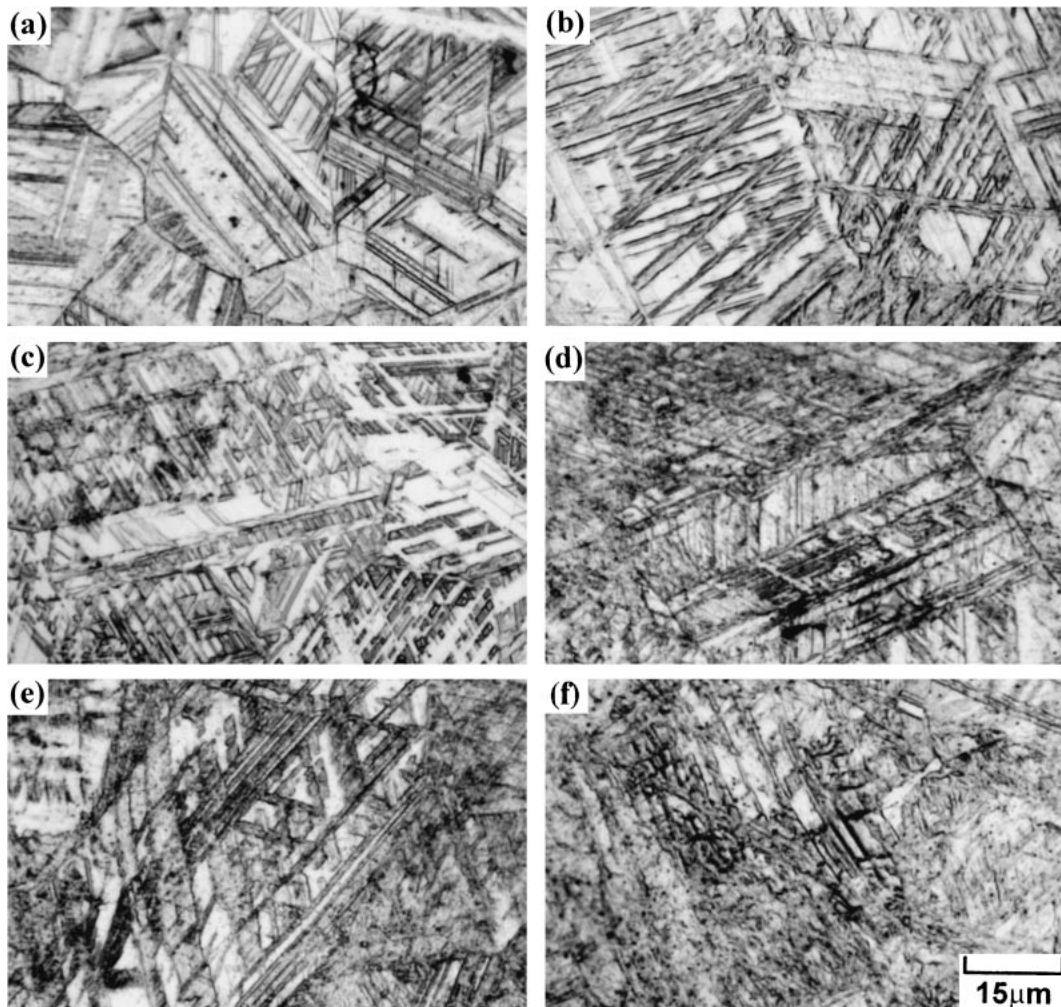


Fig. 2 Optical microstructures of Fe-22%Mn-8%Co alloy cold-rolled at various reductions in thickness. (a) 0%, (b) 5%, (c) 10%, (d) 20%, (e) 30%, (f) 50%.

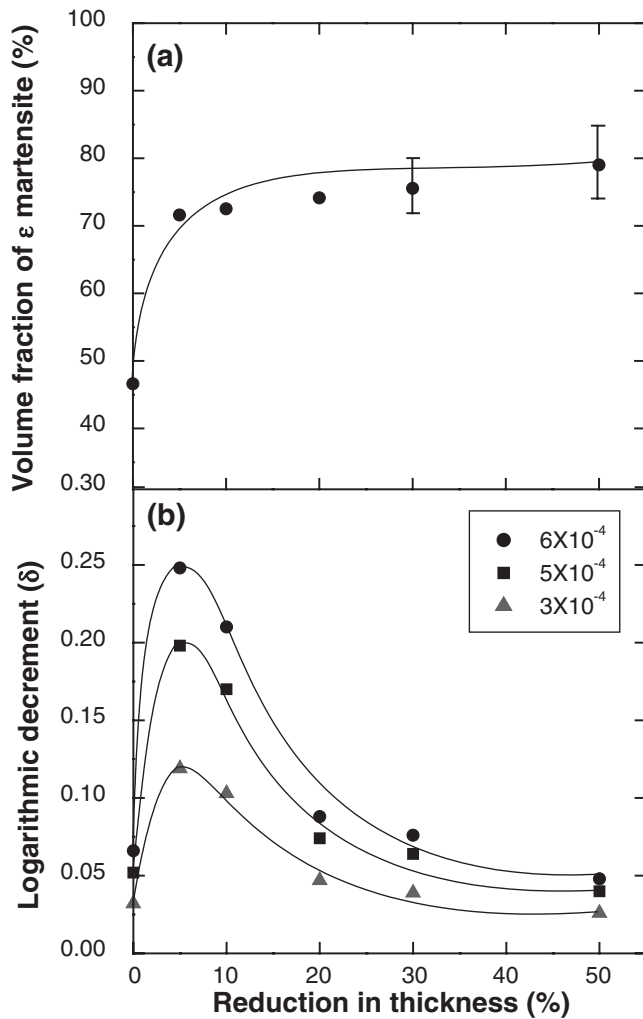


Fig. 3 Volume fraction of  $\epsilon$  martensite (a) and damping capacity (b) of Fe-22%Mn-8%Co alloy as a function of reduction in thickness.

degrees such as 30 and 50%. So, the measured volume fractions of the highly deformed specimens are inaccurate, and the errors due to the texture are several percent as the error bars indicate.

Figure 4 shows the damping capacity of the alloy as a function of strain amplitude at each reduction of thickness. The damping capacity increases linearly with increasing the strain amplitude at any reduction in thickness, suggesting that the damping mechanisms operating in the alloy are not changed with increasing the strain amplitude in a range of  $2 \times 10^{-4}$  to  $6 \times 10^{-4}$ .

Figure 3(b) shows a plot of the damping capacity versus the reduction in thickness. The damping capacity shows a maximum at around 5% deformation and decreases with further deformation at each strain amplitude.

In order to analyse the reason that the damping capacity decreases above 5% deformation in spite of the increased  $\epsilon$  martensite content, the hardness test and TEM observation were carried out. As shown in Fig. 5, the hardness data points of the thermal martensites and 5% deformed specimen are located on a straight line (A–B). However, the hardness of all the deformed specimens except for the 5%-deformed specimen are much higher than the extended line (B–C). The

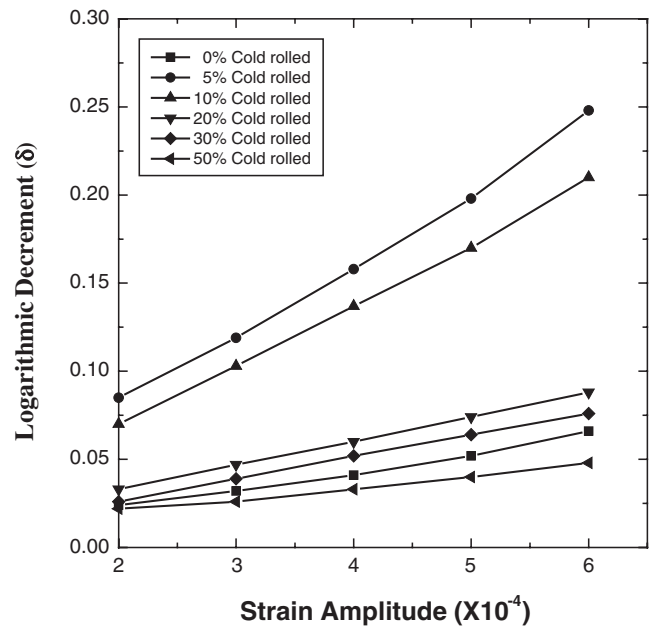


Fig. 4 Damping capacity of Fe-22%Mn-8%Co alloy as a function of strain amplitude.

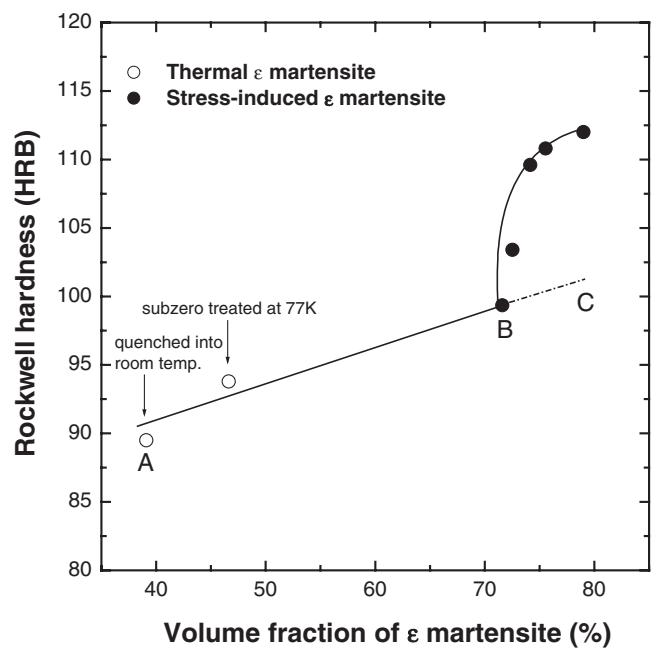


Fig. 5 Relation between hardness and volume fraction of  $\epsilon$  martensite in Fe-22%Mn-8%Co alloy.

reason is presumably ascribed to production of dislocations besides the formation of stress-induced  $\epsilon$  martensite during deformation beyond 5%. As shown in Fig. 6, it is actually observed that the density of dislocations becomes higher with increasing deformation. Therefore, the cause for the decrease of damping capacity with increasing deformation degree above 5% is that the dislocations introduced during deformation obstruct the movement of damping sources associated with  $\epsilon$  martensite, such as stacking fault boundary in  $\epsilon$  martensite and  $\gamma/\epsilon$  interface.<sup>2)</sup>

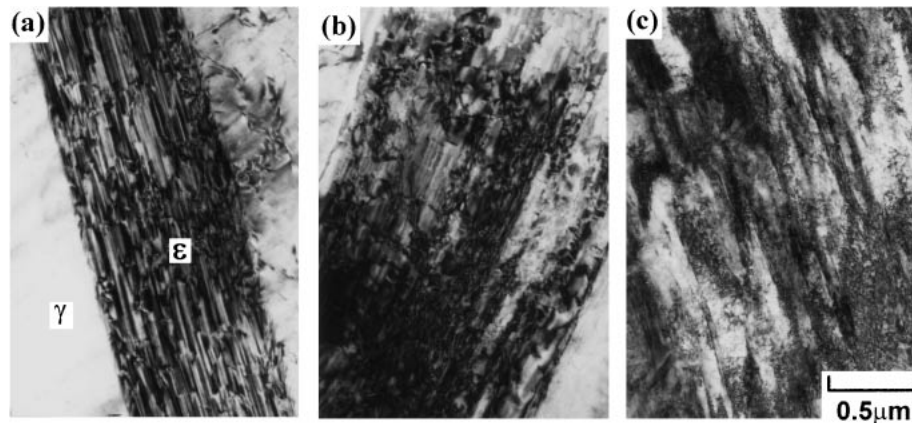


Fig. 6 Transmission electron micrographs of Fe–22%Mn–8%Co alloy subjected to various deformation degrees. (a) 10%, (b) 30%, (c) 50%.

#### 4. Conclusion

The effect of deformation on the damping capacity of Fe–22%Mn–8%Co alloy was investigated, and the results obtained in this study are summarized as follows.

- (1) The  $\gamma \rightarrow \epsilon$  stress-induced martensitic transformation occurs during deformation in the alloy without formation of  $\alpha'$  (bcc) martensite.
- (2) The amount of  $\epsilon$  martensite increases rapidly up to 5% deformation, and gradually increases with further deformation.
- (3) The damping capacity of the alloy exhibits a maximum at around 5% deformation, and decreases with further deformation in spite of the increase in  $\epsilon$  martensite content. The deterioration of damping capacity beyond 5% is ascribed to the dislocations introduced during deformation, which obstruct the movement of damping sources of the alloy.

#### REFERENCES

- 1) Y. K. Lee, J. H. Jun and C. S. Choi: *Scr. Mater.* **35** (1996) 825–830.
- 2) Y. K. Lee, J. H. Jun and C. S. Choi: *ISIJ Int.* **37** (1997) 1023–1030.
- 3) J. H. Jun and C. S. Choi: *Scr. Mater.* **38** (1998) 543–549.
- 4) J. H. Jun, Y. K. Lee and C. S. Choi: *Mater. Sci. Technol.* **16** (2000) 389–392.
- 5) H. C. Shin, J. H. Jun and C. S. Choi: *Scr. Mater.* **42** (2000) 981–986.
- 6) J. H. Jun, T. J. Ha and C. S. Choi: *Scr. Mater.* **43** (2000) 603–608.
- 7) Y. S. Seo, Y. K. Lee, and C. S. Choi: *Mater. Trans.* **44** (2003) 931–934.
- 8) Y. S. Seo, Y. K. Lee, and C. S. Choi: *Mater. Trans.* **45** (2004) 457–460.
- 9) H. Okada, H. Sahashi, N. Igata and K. Miyahara: *J. Alloys Compd.* **355** (2003) 17–21.
- 10) J. H. Jun, D. K. Kong and C. S. Choi: *Mater. Res. Bull.* **13** (1998) 1419–1425.
- 11) J. Burk and D.W. Harvey: *J. Iron Steel Inst.* **208** (1970) 779–780.
- 12) B. I. Averbach and M. Cohen: *Trans. AIME* **176** (1948) 401–415.
- 13) Y. K. Lee, S. H. Baik, J. C. Kim and C. S. Choi: *J. Alloys Compd.* **355** (2003) 10–16.
- 14) B. D. Cullity: *Elements of X-ray Diffraction*, (Addison-Wesley, Reading, Mass. 1956).